Singularities and Undefinitions in the Calibration Functions of Sonic Anemometers

ALVARO CUERVA AND ANGEL SANZ-ANDRÉS

Universidad Politécnica de Madrid, E.T.S.I. Aeronáuticos, Madrid, Spain

OSCAR LÓPEZ

IIT, Universidad Pontificia de Comillas, Madrid, Spain

(Manuscript received 15 September 2003, in final form 22 April 2004)

ABSTRACT

A mathematical model of the process employed by a sonic anemometer to build up the measured wind vector in a steady flow is presented to illustrate the way the geometry of these sensors as well as the characteristics of aerodynamic disturbance on the acoustic path can lead to singularities in the transformation function that relates the measured (disturbed) wind vector with the real (corrected) wind vector, impeding the application of correction/calibration functions for some wind conditions. An implicit function theorem allows for the identification of those combinations of real wind conditions and design parameters that lead to undefined correction/calibration functions. In general, orthogonal path sensors do not show problematic combination of parameters. However, some geometric sonic sensor designs, available in the market, with paths forming smaller angles could lead to undefined correction functions for some levels of aerodynamic disturbances and for certain wind directions. The parameters studied have a strong influence on the existence and number of singularities in the correction/calibration function as well as on the number of singularities for some combination of parameters. Some conclusions concerning good design practices are included.

1. Introduction

Sonic anemometry has now been used for more than 60 years (Suomi 1957). A remarkable improvement in sensor design and performances has taken place during recent years (Cuerva and Sanz Andrés 1999). This technology is extensively used in meteorology (Kaimal and Wyngaard 1990), wind engineering (Kato et al. 1992), industrial aerodynamics (Casten et al. 1993), wind energy (Cuerva and López Diez 1999), and space technology (Cuerva and Sanz-Andrés 2003a,b).

All of these disciplines require increasingly precise measurements. This fact has lead to the need of improving the sonic anemometer technology, in terms of sensor design, data analysis and assessment, and calibration procedures.

Sonic anemometer technology presents several advantages compared to cup anemometry. For instance, sonic anemometers can measure the three components of the wind speed vector at high effective sampling rates and only need one initial calibration and a very low maintenance effort. In addition, they are more robust than hot wire anemometers and therefore more adequate for outdoor applications (Cervenka 1992).

Corresponding author address: Dr. Alvaro Cuerva, Universidad Politécnica de Madrid, E.T.S.I. Aeronáuticos, 28040 Madrid, Spain. E-mail: acuerva@idr.upm.es

Sonic anemometers, however, present some problems associated with the measurement of mean wind characteristics such as the mean wind speed modulus or the wind direction (Grelle and Lindroth 1994; Baker et al. 1989; Heinemann et al. 1998) and the turbulent characteristics (Kaimal 1978; Silverman 1968). The measurement of the mean wind characteristics is mainly affected by aerodynamic disturbances produced by sensor struts and transducer heads (Baker et al. 1989). These disturbances can lead to acceleration or deceleration on the wind speed component along each path (Weiser and Fiedler 2001) and therefore underestimation or overestimation of the wind speed modulus and the distortion of the wind direction and the wind inclination. These distortions change with both azimuth and elevation angles.

Measurements of the turbulence are affected by aerodynamic disturbances (Wyngaard and Zhang 1985) but also, in a significant way, by the sensor measuring process itself. The measurement process can give rise to underestimation or overestimation of the turbulent wind speed components depending on their frequency, the geometry of the sensor, the Mach number of the flow, and the operational characteristic of the sensor (Cuerva and Sanz-Andrés 2003a).

With increasing use of sonic anemometers in wind energy applications, the correction of distorted mea-

surements of the mean values of wind speed measurements by means of correction functions determined in wind tunnels (Mortensen 1994) or by modeling is becoming of great importance.

In a wind tunnel, the measured wind speed modulus, wind direction, and wind inclination are compared with reference values in a process whereby the sonic is tested at different azimuth and tilt angles as well as at different wind speeds (Baker et al. 1989). Once the relation between the measured (distorted) and the real values is established, the inverse relation is calculated to correct the values to be measured in the field.

However, for some sensor designs (defined mainly by the geometry and the characteristics of aerodynamic disturbances of the sensor structure) the relation between real and measured (distorted) values could not be biyective for certain wind conditions (defined by the modulus, direction, and inclination of the wind speed vector). This means that, under some conditions, one measured magnitude could correspond to more than one real magnitude, making the application of the correction functions ineffective.

To illustrate this statement, a mathematical model of the measurement process of a sonic anemometer that takes into account the effect of the wake of a body (e.g., a sensor head wake) on the wind speed deficit along the acoustic path has been developed. A two-path sonic model is studied in order to simplify the mathematical formulation and clarify the interpretation of the results. The problem associated with the transformation of the measured (distorted) wind vector to the real wind vector is studied.

We will consider that most of the aerodynamic perturbations of the flow field in the measurement volume of the sonic anemometer can be characterized as a wake generated by an uniform incoming flow impinging on a bluff body. We will consider that the wakes of different sonic anemometer elements are not coupled to each other and, therefore, the effect of each wake element can be considered isolated. In the absence of these perturbations the correction function is the identity. As singular points in the correction function arise from the local behavior of the correction function, in an introductory work such as this paper, the study of the effect of just one wake is considered, showing the influence and relevance of the parameters involved. For aerodynamic perturbations showing a different attenuation curve, a similar analysis following the method explained here should be performed.

2. Definition of the problem

The geometry of the probe is defined by the orientation of the two paths $\mathbf{l}_1$ and $\mathbf{l}_2$ (l being the length of both paths), in an orthogonal reference system $\{\mathbf{O}_s, \mathbf{x}_s, \mathbf{y}_s\}$, attached to the sonic anemometer. The path $\mathbf{l}_1$ is aligned with the axis $\mathbf{x}_s$ and the path $\mathbf{l}_2$ forms an angle $\Delta\theta$ with the path $\mathbf{l}_1$ and therefore with the axis $\mathbf{x}_s$. Considering the previous definitions, the paths $\mathbf{l}_1$ and $\mathbf{l}_2$ can be expressed in $\{\mathbf{O}_s, \mathbf{x}_s, \mathbf{y}_s\}$ as follows:

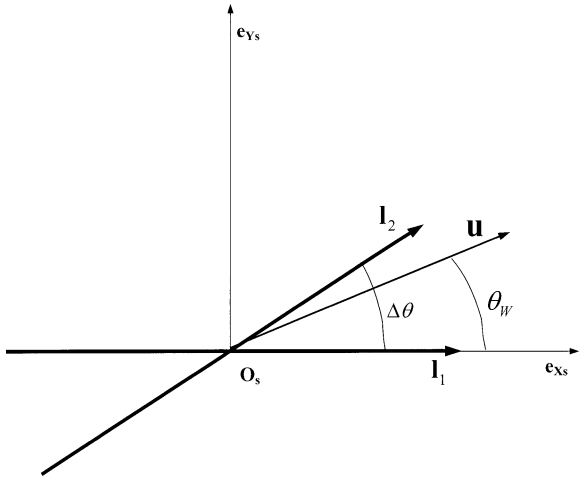

FIG. 1. Sketch of the two acoustic paths ($\mathbf{l}_1$ and $\mathbf{l}_2$) of the sonic anemometer defined in the anemometer attached reference system $\{\mathbf{O}_s, \mathbf{x}_s, \mathbf{y}_s\}$: θ_W is the real wind direction expressed in the anemometer attached reference system, $\Delta\theta$ is the angle formed by both acoustic paths, $\mathbf{e}_{x_s}$ and $\mathbf{e}_{y_s}$ are the unit vectors along the $\mathbf{x}_s$ and $\mathbf{y}_s$ axes, and $\mathbf{u}$ is the wind speed vector.

$$\begin{aligned} \mathbf{l}_1 &= l\mathbf{e}_{x_s} \\ \mathbf{l}_2 &= l[\cos(\Delta\theta)\mathbf{e}_{x_s} + \sin(\Delta\theta)\mathbf{e}_{y_s}]. \end{aligned} \tag{1}$$

Additionally, the incident wind speed vector is also expressed in $\{\mathbf{O}_s, \mathbf{x}_s, \mathbf{y}_s\}$ as

$$\mathbf{u} = |\mathbf{u}|[\cos(\theta_W)\mathbf{e}_{x_s} + \sin(\theta_W)\mathbf{e}_{y_s}], \tag{2}$$

where θ_W is the angle formed by the wind speed vector and the axis $\mathbf{x}_s$. The geometry of the problem is described in Fig. 1.

3. Sonic measuring process

In this part of the paper the measured values of the wind vector are modeled considering a steady case in presence of aerodynamic disturbances due to the structure of the sensor. A sonic anemometer measures the projection of wind speed vector along its two acoustic paths. This is done by measuring the transit times of pulses traveling from one transducer to another and vice versa (Kaimal 1978) and applying the classical time inverse algorithm. The projection of the wind speed vector on each acoustic path is given by

$$\begin{aligned} u_{l1} &= \frac{1}{l}\mathbf{u}\cdot\mathbf{l}_1 = |\mathbf{u}|\cos(\theta_w) \\ u_{l2} &= \frac{1}{l}\mathbf{u}\cdot\mathbf{l}_2 = |\mathbf{u}|[\cos(\theta_w)\cos(\Delta\theta) + \sin(\theta_w)\sin(\Delta\theta)] \\ &= |\mathbf{u}|\cos(\theta_w - \Delta\theta). \end{aligned} \tag{3}$$

The aerodynamic disturbance of sonic anemometer

measurements due to their own structure is highly complex. It results from a combination of decelerating and accelerating effects on the flow along acoustic paths. The decelerating effects are due to wakes from transducer heads and other parts of the sensor structure, whereas the acceleration effects are due to aerodynamic potential effects. Previous disturbances can be induced by the structure of one acoustic path on itself or can be a cross-disturbance of one path structure on another. Therefore, the relation of the measured (disturbed) to the real (undisturbed) wind speed component along one acoustic path can be quite complex and it is, in general, dependent on the undisturbed wind direction relative to the sensor and the wind speed modulus. Additionally, this relation is always a function of the sensor design and normally requires a specific parameterization for each sonic anemometer model.

Despite the complexity described here, the relation between the measured (disturbed) to the real (undisturbed) wind speed component along each acoustic path can be written as $u_{ls}^{M}/u_{ls} = f_{As}(\theta_{\mathrm{WPs}}, \text{geometry})$, where θ_{WPs} is the angle formed by the acoustic path and the undisturbed speed, and ''geometry'' represents appropriate design parameters.

Without any loss of generality in this treatment, and in order to reduce the complexity of the mathematics, the only aerodynamic disturbances considered here are the wakes from the traducer heads, which lead to attenuation of the measurements (Wyngaard and Zhang 1985) wind speed projections along each acoustic path. The authors are aware that a complete consideration of all disturbing sources would be needed if a full systematic study of an specific sonic anemometer is undertaken; however, this is out of the scope of this paper and is left for future works. In the case of transducer head wakes, their effects on the acoustic paths have been a main subject of concern in the literature. Several wind tunnel tests have been devoted to obtain experimental data (Weiser and Fiedler 2001; Grelle and Lindroth 1994; Mortensen 1994). These experimental data have been the source for further fitted models such as the ones proposed in Kaimal (1978) and in Wyngaard and Zhang (1985).

Although the method proposed is valid for any shape of distortion function, in this paper the distortion function derived in Wyngaard and Zhang (1985) for streamlined transducers is used as an example. Using any other distortion model (which is dependent on the analyzed sonic anemometer) does not mean any modification of the treatment of the problem. The Wyngaard model for streamlined transducers quantifies the wind speed deficit along the path as a function of the angle formed by the acoustic path and wind speed, θ_{WPs}, a minimum ratio of measured to real wind speed component along a path C and a fitting parameter a, as follows:

$$f_{As} = \frac{u_{ls}^{M}}{u_{ls}} = \{1 - (1 - C)\exp[-a\sin^2(\theta_{\mathrm{WPs}})]\}, \quad (4)$$

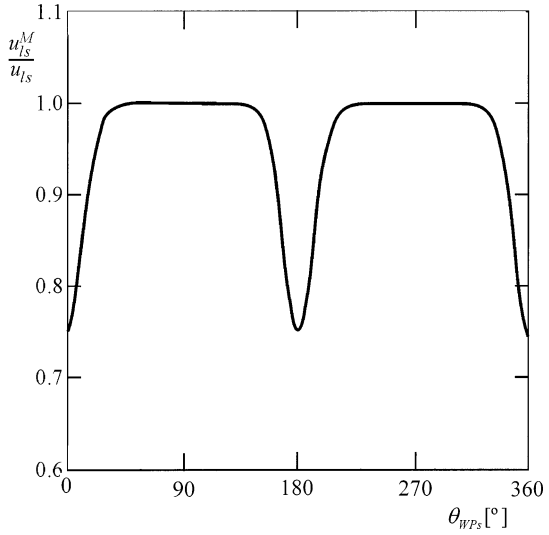

FIG. 2. Ratio of the modeled measured (distorted) to the real wind speed component along an acoustic path, u_{ls}^{M}/u_{ls}, in the range $[0, 2\pi]$ of the angle between the wind speed vector and the acoustic path, θ_{WPs}. Maximum speed attenuation parameter, $C = 0.75$. Aerodynamic angular attenuation parameter, $a = 11.5$ (characteristic angle of the region affected by the sensor head wake, $\theta_C = 0.3$ rad $\cong 17°$). (Hanafusa et al. 1980; Wyngaard and Zhang 1985).

where the superscript M stand for measured values, the angle θ_{WPs} is easily calculated as

$$\theta_{\mathrm{WPs}} = \arccos\left(\frac{u_{ls}}{|\mathbf{u}|}\right), \quad (5)$$

and the parameter C depends on the ratio l/d. Here d is the equivalent diameter of the head transducer. Some authors have stated a dependency of C on wind speed. From (4) it is easily identified that $(1 - C)$ is the value of maximum attenuation (when the wind speed vector is aligned with the acoustic path). The parameter a controls the width of the nondisturbed angular interval (plateau of the curve in Fig. 2). The affected angular interval is measured by the characteristic angle:

$$\theta_C = \arcsin\frac{1}{\sqrt{a}}. \quad (6)$$

In the present case,

$$\theta_{\mathrm{WP}_1} = \theta_w$$

$$\theta_{\mathrm{WP}_2} = \arccos[\cos(\theta_w)\cos(\Delta\theta) + \sin(\theta_w)\sin(\Delta\theta)]$$

$$= -(\theta_w - \Delta\theta). \quad (7)$$

Figure 2 shows the dependency of the attenuation function $f_A S$, given by (4) for both paths in the range of wind speed direction $\theta_W[0 - 2\pi]$.

Once the attenuation functions are calculated, it is possible to obtain the measured values along each path as follows:

$$u_{ls}^{M} = f_{As}u_{ls}. \quad (8)$$

As u_{ls}^M are, in fact, obtained from one model of the measuring process, they will be denoted as ''modeled measured wind speed components.''

From the modeled measured speed components expressed in the $\{\mathbf{O}_s, \mathbf{x}_s, \mathbf{y}_s\}$ reference system it is possible to obtain the modeled wind speed values along each acoustic path based on the transformation relationship between the two reference systems, given by

$$\begin{Bmatrix} u_{l1} \\ u_{l2} \end{Bmatrix} = \begin{bmatrix} 1 & 0 \\ \cos(\Delta\theta) & \sin(\Delta\theta) \end{bmatrix} \begin{Bmatrix} u_{XS} \\ u_{YS} \end{Bmatrix}. \tag{9}$$

The inverse relation of (9) is applied to obtain the modeled measured components of wind speed in the $\{\mathbf{O}_s, \mathbf{x}_s, \mathbf{y}_s\}$ reference system from the components along each acoustic path

$$\begin{Bmatrix} u_{XS}^M \\ u_{YS}^M \end{Bmatrix} \begin{bmatrix} 1 & 0 \\ -\dfrac{\cos(\Delta\theta)}{\sin(\Delta\theta)} & \dfrac{1}{\sin(\Delta\theta)} \end{bmatrix} \begin{Bmatrix} u_{l1}^M \\ u_{l2}^M \end{Bmatrix}. \tag{10}$$

The modeled measured values of wind speed modulus and direction are obtained from the wind speed modeled measured components in the $\{\mathbf{O}_s, \mathbf{x}_s, \mathbf{y}_s\}$ reference system as follows:

$$\begin{aligned} u_W^M &= [(u_{XS}^M)^2 + (u_{YS}^M)^2]^{1/2}, \\ \theta_W^M &= \arctan\left(\frac{u_{YS}^M}{u_{XS}^M}\right)_{-\pi,\pi}. \end{aligned} \tag{11}$$

Once the modeled measured wind speed modulus and direction are obtained, it is possible to establish a general function $\mathbf{F}$ between the variables involved in the problem,

$$\mathbf{F}: \mathbb{R}^5 \to \mathbb{R}^2: \{u_W, \theta_W, C, a, \Delta\theta\} \to \{u_W^M, \theta_W^M\}, \tag{12}$$

the domains for each component being as follows:

$$\begin{aligned} u_W &\in (0, 100)\ (\mathrm{m\ s^{-1}}) \\ \theta_W &\in (0, 2\pi)\ (\mathrm{rad}) \\ C &\in (0.5, 1) \\ \Delta\theta &\in (0, 2\pi)\ (\mathrm{rad}) \\ a &\in (5, 15), \end{aligned}$$

based on the experience with sonic anemometers. Basic initial assumptions have been made when defining the previous domains. A first remark can be pointed out based on experimental observations. Attenuation values, C, from literature are remarkably above 0, and values between $C = 0.5$ and $C = 0.9$ can be considered. Typical values about 10 are found for a ($\theta_C = 0.32$ rad $\cong 18°$). Parameter $\Delta\theta$ is normally 90°, although some models present a value of 60°. In this paper the full domains are considered since one of our goals is to establish the consequences of practical limits of such design parameters.

4. The transformation function

The function $\mathbf{F}$ can be determined experimentally in wind tunnels or by application of models, as has been done here. In that case, parameters C, a, and $\Delta\theta$ are already defined. Once the function is obtained, in what can be denoted a calibration or assessment process, it is necessary to obtain its inverse $\mathbf{F}^{-1}$ since this inverse function will be applied to correct the measured data produced by sonic anemometers in the real field when the real values must be obtained from measured values (which are distorted by the aerodynamic perturbations).

As it is well known from the implict function theorem, the calculation of $\mathbf{F}^{-1}$ may lead to problems in cases where the Jacobian matrix of the transformation is singular. In such a case, the correction process (by applying $\mathbf{F}^{-1}$ to the measured values) is not possible. To study these situations with the model presented here, C, a, and $\Delta\theta$ are considered known parameters, which for some real wind conditions (u_W and θ_W) could lead to an undefined $\mathbf{F}^{-1}$.

The Jacobian matrix for the transformation $\mathbf{F}$, considering C, a, and $\Delta\theta$ as parameters, is expressed in the following way:

$$\mathbf{J}_\mathbf{F}(u_W, \theta_W; C, a, \Delta\theta) = \begin{bmatrix} \dfrac{\partial u_W^M}{\partial u_W} & \dfrac{\partial u_W^M}{\partial \theta_W} \\ \dfrac{\partial \theta_W^M}{\partial u_W} & \dfrac{\partial \theta_W^M}{\partial \theta_W} \end{bmatrix}. \tag{13}$$

The points $\{u_W, \theta_W, C, a, \Delta\theta\}$, where the determinant of the Jacobian matrix of $\mathbf{F}$ is zero, are studied because the transformation $\mathbf{F}$ (or its inverse, $\mathbf{F}^{-1}$) will show singular points (the transformation will not be defined at these points).

In expression (13) the partial derivative of the measured wind direction versus the real wind speed is zero; therefore, $\det[\mathbf{J}_\mathbf{F}] = 0$ reduces to

$$\det[\mathbf{J}_\mathbf{F}] = 0 \Leftrightarrow \frac{\partial u_W^M}{\partial u_W}\frac{\partial \theta_W^M}{\partial \theta_W} = 0. \tag{14}$$

This is only true for the considered formulation of the aerodynamic disturbances (C and a independent from wind speed modulus). The previous reasoning allows one to eliminate u_W from the list of parameters influencing the singularity analysis. Additionally, for this problem, it is established that the partial derivative of the measured wind speed modulus versus real wind speed modulus is a function of θ_W, C, a, and $\Delta\theta$, which never becomes 0. In this situation, singular points of the transformation are given by

$$\det[\mathbf{J}_\mathbf{F}] = 0 \Leftrightarrow \frac{\partial \theta_W^M}{\partial \theta_W}(\theta_W, C, a, \Delta\theta) = 0. \tag{15}$$

In Fig. 3 the surface implicitly defined by (15) is shown for $a = 10$ ($\theta_C = 0.32$ rad $\cong 18°$). In all the points $(\theta_W, C, \Delta\theta)$ belonging to the mentioned surface, the correction function $\mathbf{F}^{-1}$ is not defined, and therefore

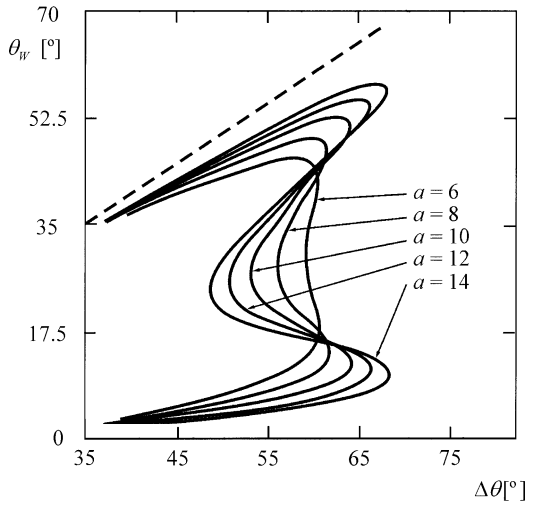

FIG. 3. Variation of the wind direction θ_w, with the angle between the acoustic paths, $\Delta\theta$, for different values of the aerodynamic angular attenuation parameter, a, that makes singular the transformation from the real to the measured values (det[$\mathbf{J_F}$] = 0) for a maximum speed attenuation parameter, $C = 0.6$. Dashed line: $\theta_w = \Delta\theta$ [asymptotic behavior of $\theta_w(\Delta\theta)$ curve].

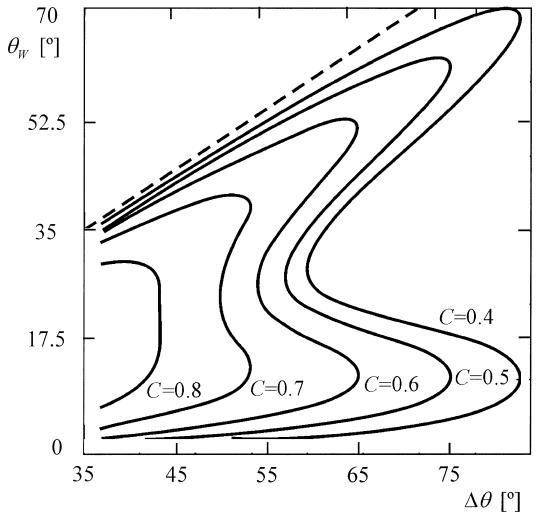

FIG. 4. Variation of the wind direction θ_w with the angle between the acoustic paths, $\Delta\theta$, for different values of the maximum speed attenuation parameter C that makes singular the transformation from the real to the measured values (det[$\mathbf{J_F}$] = 0) (aerodynamic angular attenuation parameter, $a = 10$ that is characteristic angle of the region affected, $\theta_C = 0.32$ rad $\cong 18°$). Dashed line: $\theta_w = \Delta\theta$ [asymptotic behavior of $\theta_w(\Delta\theta)$ curve].

the correction of measured data for such values would not be possible. A similar analysis for those points (θ_W, a, $\Delta\theta$) that make det[$\mathbf{J_F}$] = 0 for a typical value $C = 0.6$ gives rise to the results shown in Fig. 4.

From Figs. 3 and 4 it can be derived that θ_W, C, a, and $\Delta\theta$ are the driving parameters leading to undefinitions in the determination of correction function $\mathbf{F}^{-1}$ for some conditions. It is remarkable (see Fig. 4) that for higher values of C (lower attenuations) only two problematic real wind directions appear within the $\theta_W \in [0°, 90°]$ range studied for a given geometry $\Delta\theta$. However, decreasing the values of C (higher attenuations) gives rise to four critical wind directions within the mentioned interval. As can be observed, there is a strong mutual dependence among the values of the parameters that give rise to singularities in the calibration function.

Two critical points correspond to θ_W close to $\theta_W = 0°$ and the asymptote $\theta_W = \Delta\theta$, as could be expected. For given wind conditions (given θ_W), the condition det[$\mathbf{J_F}$] = 0 defines a surface in R^3 that relates those design values $\{C, a, \Delta\theta\}$, giving rise to singularities in the transformation for those wind conditions. Figure 5 shows this surface (in terms of level curves) when $\theta_W = 45°$. Figure 5 indicates that larger values of a (larger angles between the acoustic path and the wind speed vector without attenuations) require decreasing values of $\Delta\theta$ to lead to singular points in the correction function. A similar conclusion is established for decreasing maximum attenuations (increasing C values). In general, it can be stated that the intuitively better situation, orthogonal paths $\Delta\theta = 90°$, combined with typical values for a ($\approx$10) and C ($\approx$0.7) does not give rise to singular situations for the studied case. Those points presented in previous curves associated with singularities in the correction function $\mathbf{F}^{-1}$ give rise to nondetermination of such a correction function.

In Fig. 6 the values of the modeled real wind direction for a given geometry $\Delta\theta = 60°$ and the parameter $a = 10$ are represented as a function of the real wind speed direction θ_W and of the speed attenuation parameter C. Observe that the line $C = 1$ represents the no-attenuation case. The orientation $\theta_W = 30°$ is the half-angle

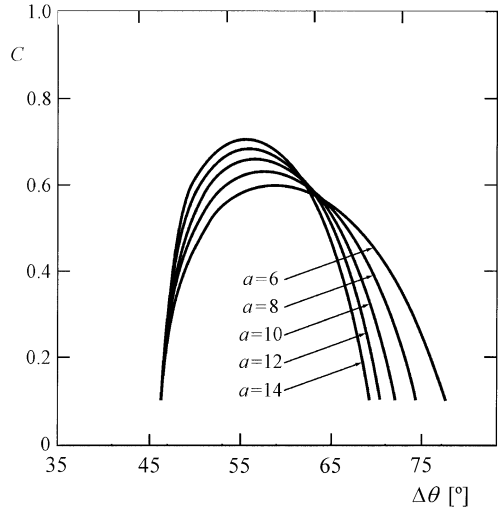

FIG. 5. Variation of the maximum speed attenuation parameter C with the angle between the acoustic paths, $\Delta\theta$, for different values of the aerodynamic angular attenuation parameter a that makes singular the transformation from the real to the measured values (det[$\mathbf{J_F}$] = 0) for a given wind direction, $\theta_W = 45°$.

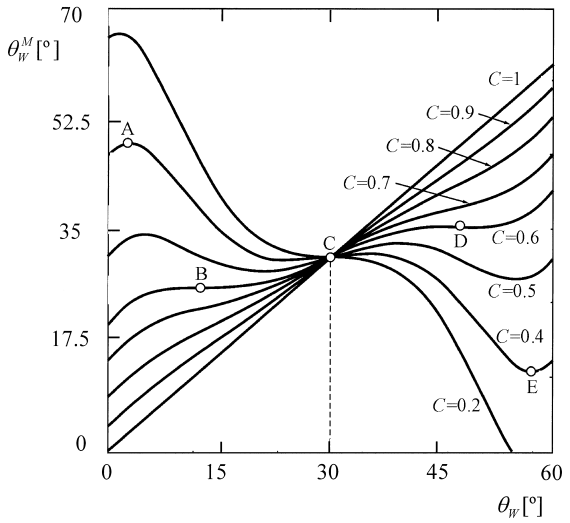

FIG. 6. Values of the modeled measured wind direction expressed in a sonic anemometer reference system, θ_W^M, as function of real wind speed direction θ_W and the maximum speed attenuation parameter C for a given angle between the acoustic paths, $\Delta\theta = 60°$, and an aerodynamic angular attenuation parameter, $a = 10$ (characteristic angle of the region affected, $\theta_C = 0.32$ rad $\cong 18°$).

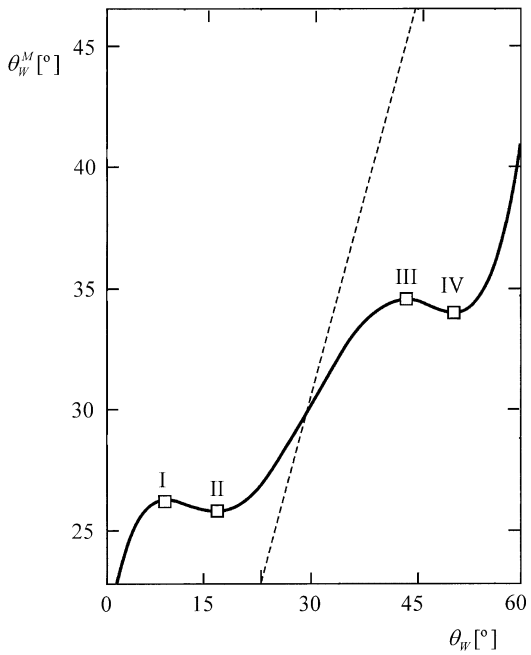

FIG. 8. Relation between the modeled measured wind direction expressed in a sonic anemometer reference system, θ_W^M, and the real wind speed direction, θ_W for a given angle between acoustic paths, $\Delta\theta = 60°$, an aerodynamic attenuation parameter, $a = 10$ (characteristic angle of the region affected by the sensor head wake, $\theta_C = 0.32$ rad $\cong 18°$), and a minimum ratio of the modeled measured to the real wind speed component along the acoustic paths, $C = 0.55$. Dashed lines indicate the ideal relation (straight line with zero offset and unity slope).

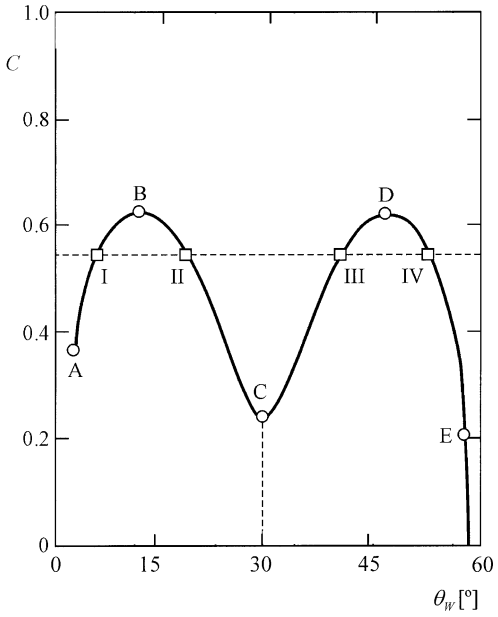

FIG. 7. Values of the minimum ratio of the modeled measured to the real wind speed component along the acoustic paths, C, and the real wind speed direction θ_W giving rise to singularities ($\det[\mathbf{J_F}] = 0$) in the calibration functions for a given angle between the acoustic paths, $\Delta\theta = 60°$, and an aerodynamic angular attenuation parameter, $a = 10$ (characteristic angle of the region affected by the sensor head wake, $\theta_C = 0.32$ rad $\cong 18°$), and a maximum speed attenuation parameter, $C = 0.55$. Dashed lines indicate ideal relation (straight line $\theta_W^M = \theta_W$).

of the acoustic paths and, therefore, no distortion of θ_W^M occurs at this orientation. In this figure, a limit of the value of parameter C exists for which a given measured wind direction, θ_W^M, might correspond to three real values of the wind direction θ_W. This fact evidences the impossibility of applying the correction function $\mathbf{F}^{-1}$ for a certain range of values of θ_W^M. The range amplitude depends on the geometry, $\Delta\theta$, and on the attenuation parameter C.

The singularities on the previous surface correspond to those coordinates C, θ_W that satisfy the condition $\det[\mathbf{J_F}] = 0$ for the given conditions. The corresponding curve is presented in Fig. 7. As an example, in Fig. 7 a horizontal straight line at $C = 0.55$ allows one to identify those real wind directions in the interval [0°, 90°], giving rise to four singularities (points I, II, III, IV). In Fig. 8 a single case for the surface given in Fig. 6 is presented for the same attenuation level and $C = 0.55$. In Fig. 7 the singular points are identified by roman numbers, logically coincident with the relative extremes of the calibration function in Fig. 8. High attenuation levels ($C = 0.55$) give rise not only to singularities but also to high deviations of the modeled measured values of the wind direction from the real ones.

In Fig. 9 a zoom of Fig. 8 is included to analyze the possible influence of such singularities in a calibration

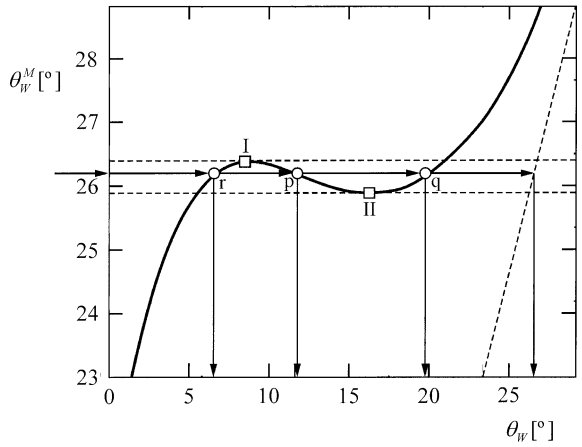

FIG. 9. Zoom of Fig. 8 close to points I and II.

process. It can be shown that for the measured wind direction values between the horizontal lines defined by I and II three corrected values are possible ($\theta_W = r$, p, or q). The physical meaning of the singularities described in the previous analysis is evident here.

5. Conclusions

The geometry of sonic anemometers as well as the characteristic of the aerodynamic disturbance produced by sonic elements on the flow crossing the acoustic path can lead to singularities in the transformation function that relates the measured (disturbed) wind speed vector with the real (corrected) wind speed vector.

The implicit function theorem allows one to identify those combinations of real wind conditions and design parameters that lead to undefined correction functions. The real wind direction is the natural parameter giving rise to singularities in the transformation between real and the measured values, for the considered formulation of aerodynamic disturbances considered (independent from wind speed modulus).

Generally speaking, the classical sensor with orthogonal paths does not show problematic regions. However, some geometrical designs, existing in the market, with the acoustic paths forming smaller angles and for certain levels of aerodynamic disturbances, could lead to undefined correction functions for some wind directions. The parameters studied here have a strong influence in the existence of singularities in the calibration/correction function as well as in the number of these singularities for certain combination of parameters.

APPENDIX

Symbols

a: Aerodynamic angular attenuation parameter.

C: Minimum ratio of the modeled measured to the real wind speed component along an acoustic path (so-called maximum speed attenuation parameter).

l: Length of an acoustic path.

$\{\mathbf{O}_s, \mathbf{x}_s, \mathbf{y}_s\}$: Sonic anemometer reference system.

d: Characteristics diameter of the transducer head.

$\mathbf{e}_{x_s}$: Unit vector along $\mathbf{x}_s$ axis.

$\mathbf{e}_{y_s}$: Unit vector along $\mathbf{y}_s$ axis.

f_{As}: Ratio of the modeled measured to the real wind speed component along an acoustic path.

$\mathbf{F}$: Transformation function between the modeled measured and the real wind speed modulus and direction.

$\mathbf{J}_\mathbf{F}$: Jacobian matrix of $\mathbf{F}$.

$\mathbf{l}_1$: Acoustic path 1.

$\mathbf{l}_2$: Acoustic path 2.

$\mathbf{u}$: Wind speed vector.

u_{ls}: Real wind speed component along an acoustic path.

u_{XS}: Real wind speed component along $\mathbf{x}_s$ axis.

u_{YS}: Real wind speed component along $\mathbf{y}_s$ axis.

u_{ls}^M: Modeled measured wind speed component along an acoustic path.

u_W: Real wind speed modulus.

u_W^M: Modeled measured wind speed modulus.

u_{XS}^M: Modeled measured wind speed component along $\mathbf{x}_s$ axis.

u_{YS}^M: Modeled measured wind speed component along $\mathbf{y}_s$ axis.

$\Delta\theta$: Angle formed between the two acoustic paths.

θ_C: Characteristic angle of the region affected by the sensor head wake.

θ_W: Real wind direction expressed in the sonic anemometer reference system.

θ_{WPs}: Angle between the wind speed vector and an acoustic path.

θ_W^M: Modeled measured wind direction expressed in the sonic anemometer reference system.

REFERENCES

Baker, C. B., R. F. Eskridge, P. S. Conclin, and K. R. Knoerr, 1989: Wind tunnel investigation of three sonic anemometers. NOAA Tech. Memo. ERL ARL-178, Air Resources Laboratory, Silver Spring, MD, 30 pp.

Casten, T., P. Mousset-Jones, and F. Calizaya, 1993: Ultrasonic anemometry in underground excavations. *Proc. Seventh Mine Ventilation Symp.*, Littleton, CO, Society for Mining, Metallurgy and Exploration, 429–433.

Cervenka, S., 1992: Selection of an anemometer for measurement of wind turbulence. ECN Tech. Rep. ECN-I-92-029 DE92 557290, 40 pp.

Cuerva, A., and S. López Diez, 1999: Higher level descriptors of sites and wind turbines by means of principal components analysis. *Proceedings of the European Wind Energy Conference*

EWEC '97, A. D. Garrad, W. Palz, and S. Scheller, Eds., James & James Science, 653–656.

——, and A. Sanz-Andrés, 1999: Steps to reach a safe scenario with sonic anemometers as standard sensor for wind measurements in wind energy. *Proceedings of the European Wind Energy Conference EWEC '97*, A. D. Garrad, W. Palz, and S. Scheller, Eds., James & James Science, 649–652.

——, and ——, 2003a: On multiple-path sonic anemometer theory. *Experiments in Fluids*, **34,** doi:10.1007/s00348-002-0565-x.

——, and ——, 2003b: Sonic anemometry of planetary atmospheres. *J. Geophys. Res.*, **108,** 5029, doi:10.1029/2002JE001944.

Grelle, A., and A. Lindroth, 1994: Flow distortion by a solent sonic anemometer: Wind tunnel calibration and its assessment for flux measurement over forest field. *J. Atmos. Oceanic Technol.*, **11,** 1529–1542.

Hanafusa, T., T. Korobi, and Y. Minutsa, 1980: Single head sonic anemometer–thermometer. Lower Tropospheric Data Compatibility Series, WMO Instruments and Observing Methods Tech. Rep. 3.

Heinemann, D., D. Laugner, U. Stahe, and H. Waldl, 1998: Measurement and correction of ultrasonic anemometer errors and impact on turbulence measurements. *Proc. European Wind Energy Conf. EWEC '97*, Dublin, United Kingdom, IWEA, 409–412.

Kaimal, J. C., 1978: Sonic Anemometer Measurement of Atmospheric Turbulence, *Dynamic Flow Conference*, Pergamon Press, 551–565.

——, and J. Wyngaard, 1990: The Kansas and Minnesota experiments. *Bound.-Layer Meteor.*, **50,** 31–47.

Kato, N., T. Okuma, J. R. Kim, H. Marukawa, and Y. Niihori, 1992: Full scale measurements of wind velocity in two urban areas using an ultrasonic anemometer. *J. Wind Eng. Industrial Aerodyn.*, **41,** 67–78.

Mortensen, N. G., 1994: Flow-response characteristics of the Kaijo Denki omni-directional sonic anemometer. RISO Tech, Rep. TR-61B, 31 pp.

Silverman, B. A., 1968: The effect of spatial averaging on spectrum estimation. *J. Appl. Meteor.*, **7,** 168–172.

Suomi, V. E., 1957: Energy budget studies and development of the sonic anemometer for spectrum analysis. *Exploring the Atmosphere's First Mile*, H. H. Lettau, Ed., Pergamon Press, 578 pp.

Weiser, A., and F. Fiedler, 2001: The influence of the sensor design on wind measurements with sonic anemometer systems. *J. Atmos. Oceanic Technol.*, **18,** 1585–1608.

Wyngaard, J., and S. Zhang, 1985: Transducer-shadow effects on turbulence spectra measured by sonic anemometers. *J. Atmos. Oceanic Technol.*, **2,** 548–558.